

—

Broadband frequency entangled photon generation using silicon nitride ring cavities

Zhengkao Yin

Abstract

Lorem ipsum dolor sit amet, consectetur adipiscing elit. Ut purus elit, vestibulum ut, placerat ac, adipiscing vitae, felis. Curabitur dictum gravida mauris. Nam arcu libero, nonummy eget, consectetur id, vulputate a, magna. Donec vehicula augue eu neque. Pellentesque habitant morbi tristique senectus et netus et malesuada fames ac turpis egestas. Mauris ut leo. Cras viverra metus rhoncus sem. Nulla et lectus vestibulum urna fringilla ultrices. Phasellus eu tellus sit amet tortor gravida placerat. Integer sapien est, iaculis in, pretium quis, viverra ac, nunc. Praesent eget sem vel leo ultrices bibendum. Aenean faucibus. Morbi dolor nulla, malesuada eu, pulvinar at, mollis ac, nulla. Curabitur auctor semper nulla. Donec varius orci eget risus. Duis nibh mi, congue eu, accumsan eleifend, sagittis quis, diam. Duis eget orci sit amet orci dignissim rutrum.

Contents

Chapter 1

Introduction

Nam dui ligula, fringilla a, euismod sodales, sollicitudin vel, wisi. Morbi auctor lorem non justo. Nam lacus libero, pretium at, lobortis vitae, ultricies et, tellus. Donec aliquet, tortor sed accumsan bibendum, erat ligula aliquet magna, vitae ornare odio metus a mi. Morbi ac orci et nisl hendrerit mollis. Suspendisse ut massa. Cras nec ante. Pellentesque a nulla. Cum sociis natoque penatibus et magnis dis parturient montes, nascetur ridiculus mus. Aliquam tincidunt urna. Nulla ullamcorper vestibulum turpis. Pellentesque cursus luctus mauris.

Nulla malesuada porttitor diam. Donec felis erat, congue non, volutpat at, tincidunt tristique, libero. Vivamus viverra fermentum felis. Donec nonummy pellentesque ante. Phasellus adipiscing semper elit. Proin fermentum massa ac quam. Sed diam turpis, molestie vitae, placerat a, molestie nec, leo. Maecenas lacinia. Nam ipsum ligula, eleifend at, accumsan nec, suscipit a, ipsum. Morbi blandit ligula feugiat magna. Nunc eleifend consequat lorem. Sed lacinia nulla vitae enim. Pellentesque tincidunt purus vel magna. Integer non enim. Praesent euismod nunc eu purus. Donec bibendum quam in tellus. Nullam cursus pulvinar lectus. Donec et mi. Nam vulputate metus eu enim. Vestibulum pellentesque felis eu massa.

1.1 BACKGROUND

1.1.1 Chip-scale quantum information processing

1.1.2 Entangled photon sources for quantum communication and sensing

1.2 CURRENT PROBLEMS

Chapter 2

Principal Theory

In chip scale quantum optical platforms, to confine the light in a sub-micron dimension, the mean how light propagate is different from the TEM mode or Gaussian mode in free space. Based on the conventional guided wave theory, the fundamental mode, which is mainly used in integrated optical applications, can be solved in some simple cases with some approximations. Furthermore, due to the broadband motivation in this study, it is essential to the dispersion into consideration, not only in the part of propagation but also the nonlinear progress where the photon pairs are generated.

In this chapter, the waveguide theory is roughly introduced and sequentially, mode coupling theory is discussed in the case of ring resonator. Second section will focus on nonlinear optics in the view of waveguide.

2.1 GUIDED MODES

In an ideal optical waveguide, the core layer and the cladding layer are usually composed of two different materials, where the refractive index is larger in the core. As an analogue of optical fibers, only in the higher index region can the light propagate, and meanwhile dissipate in a wavelength scale in the lower index region.

Usually, we assume the core and the cladding layer are made of nonmagnetic (magnetic permeability $\mu = \mu_0$) and dielectric material (conductivity $\sigma = 0$). Furthermore, we neglect the nonlinear response of the polarization of electric field ($\mathbf{P} \simeq \varepsilon_0 \chi \mathbf{E}$).

Since the waveguide in numerous research objects, is deposited or sputtered using chemical or physical methods, the uneven den-

sity in the waveguide layer can not be negligible. Hence, the propagation equation derived from Maxwell's equation is

$$(\nabla_{\perp}^2 + k^2 n^2 - \beta^2) \mathbf{E} = -(\nabla_{\perp} + i\beta \hat{\mathbf{z}})(\mathbf{E}_{\perp} \cdot \nabla_{\perp} \ln n^2) \quad (2.1)$$

where \perp denotes the transverse component, $\nabla_{\perp}^2 = \nabla_x^2 + \nabla_y^2$. And k, n, β are the wave vector in vacuum, refractive index and propagation constant, respectively. While, with the negligible film anisotropy, ?? can be approximated into

$$(\nabla_{\perp}^2 + k^2 n^2 - \beta^2) \mathbf{E} = 0 \quad (2.2)$$

This is the normal *Helmholtz equation*, indicating the relation between propagation constant β and material refractive index, i.e. *chromatic dispersion*.

Next, the boundary conditions determining the solution to Eqn. ??, arise from the Maxwell's equations as well.

$$\begin{aligned} \hat{\mathbf{n}} \cdot (\mathbf{E}_a - \mathbf{E}_b) &= 0 \\ \hat{\mathbf{n}} \times (\mathbf{H}_a - \mathbf{H}_b) &= 0 \end{aligned}$$

which is the continuity condition of both electric and magnetic field at all dielectric material interfaces. Here, $\hat{\mathbf{n}}$ is the normal direction at the material boundary and the subscript a, b denote different regions.

In the case of channel waveguides, the index discontinuity from both vertical and horizontal sides can be decomposed into two sets of independent and complete conditions, i.e. the horizontal boundary condition and vertical boundary condition, with the discontinuity on the waveguide corners neglected. In other words, approximately the equation has two independent particular solutions, which is the mathematical origin of *transverse electric* (TE) modes and *transverse magnetic* (TM) modes.

Hence, we can study the eigenequation by selecting only one set of boundary condition, as used in the *the effective index method*. For example, in a planar waveguide shown in ??, $\frac{d^2}{dy^2} = 0$ ¹, the TE mode features $E_x = 0$ and consider only y -component,

$$\frac{d^2 E_y}{dx^2} + (k^2 n^2 - \beta^2) E_y = 0 \quad (2.3)$$

¹Since the planar waveguide is infinite at the y -direction, thus the solution is identical in arbitrary xz -plane, which means no gradient along x -axis.

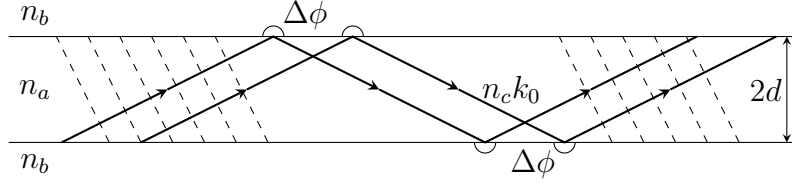


Figure 2.1: **Planar waveguide.** The upper and bottom layer are cladding and the middle is core layer. $\Delta\phi$ represents the GoosHänchen shift at the boundary.

and E_y is continuous at $x = \pm d/2$, where d is the thickness of core layer.

For the region $|x| > d/2$, the light evanesces at x -direction at rate κ and in contrast, in the region of core layer, the light performs like stationary wave, denoting with k_x . By substituting these conditions, phase continuity is achieved between two interface

$$2k_x d = m\pi + 2 \arctan(\kappa/k_x) \quad (2.4)$$

where m is the index of stationary wave. The second term can be treated as the Goos-Hänchen phase shift. Overall, the waveguide modes characterize that the phase shall maintain itself with an $m\pi$ shift along with the shift at the boundaries.

In the case of TM modes, the eigen equation is

$$2k_x d = m\pi + 2 \arctan(\delta\kappa/k_x) \quad (2.5)$$

where $\delta = n_a/n_b$ is the index ratio and only differs from ?? with this parameter. conclusively, the less is δ parameter, the propagation constant of TE and TM modes are closer.

2.2 RING RESONATORS

The working principle of ring resonator can be derived completely [?] as an analogue to Fabry-Pérot etalon, based on the coupling mode theory. In the model illustrated in ??, the self-coupling coefficient τ and the cross-coupling coefficient κ can be evaluated analytically or using numerical simulation. Assuming the coupling only occur at the very close area, τ, κ are the power splitting ratios of the coupler and satisfy $\tau^2 + \kappa^2 = 1$ if the coupling section is lossless. a is

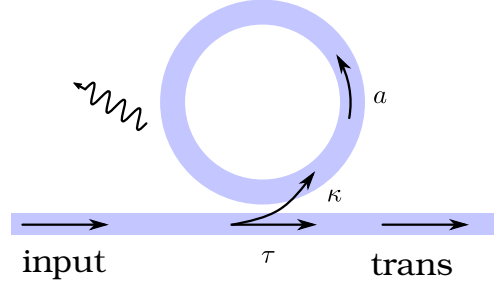


Figure 2.2: **An all-pass type ring resonator.** The transmitted spectrum is filtered periodically by the ring waveguide, in the case satisfying resonance condition.

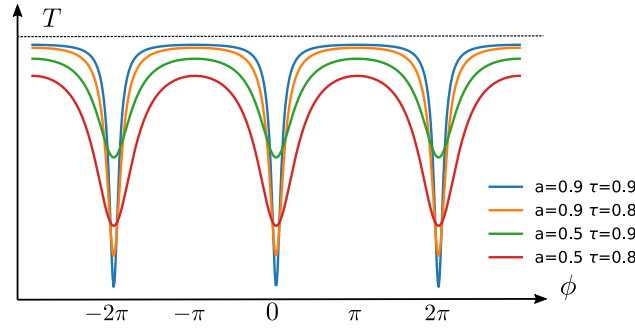


Figure 2.3: **The transmission spectrum of a ring resonator.**

the single-pass amplitude transmission, including both propagation loss in the ring and loss in the couplers.

The transmission rate of a all-pass type ring cavity takes the form of

$$T = \frac{I_{\text{pass}}}{I_{\text{input}}} = \frac{a^2 - 2a\tau \cos \phi + \tau^2}{1 - 2a\tau \cos \phi + a^2\tau^2} \quad (2.6)$$

Here $\phi = \beta L$ is the phase shift in a single round trip. The transmission rate is plotted as a function of phase ϕ

In ??, first, the resonance can be achieved as $\phi = 2\mu\pi$ leads to the minima of T_n , shown in. Hence

$$\beta L = 2\mu\pi \quad (2.7)$$

is the resonance condition.

Meanwhile, $a = \tau$, where the input power can compensate the loss of one round trip propagation.

In , we can see the spectral characteristics is periodical. The extinction ratio of absorption peak is defined by a, τ . From ??, we

can derive the full width at half maximum (FWHM) of the resonance spectrum

$$\delta\phi = \frac{2(1 - a\tau)}{\sqrt{\tau a}} \quad (2.8)$$

thus the half width of wavelength and frequency are

$$\delta\lambda = \frac{2(1 - a\tau)}{\sqrt{\tau a}} \quad (2.9)$$

And the finesse F of the resonator is defined as

$$F \equiv \frac{2\pi}{\delta\phi} = \quad (2.10)$$

2.3 DEGENERATE FOUR WAVE MIXING

In addition, in the case of nonlinear photonics, the nonlinear response of the electric field is inherent and essential, hence we also derive the propagation by treating the nonlinear term as an additive source.

In addition, in the case of nonlinear photonics, the nonlinear response of the electric field is inherent and essential, hence we also derive the propagation by treating the nonlinear term as an additive source.

2.4 INTEGRATED NONLINEAR DEVICE

Chapter 3

Phase match condition for spontaneous four wave mixing in a ring cavity

3.1 CHROMATIC DISPERSION

3.2 BROADBAND PHASE MATCHING CONDITION

3.3 DISPERSION COMPENSATION AND ENGINEERING USING SLOT STRUCTURE

3.4 EFFECTS OF MODE CROSSING

3.5 FOUR WAVE MIXING

Assume in a ring resonator, to satisfy both energy conservation and momentum conservation,

$$\begin{aligned}\beta_i + \beta_s &= 2\beta_p \\ \omega_i + \omega_s &= 2\omega_p\end{aligned}$$

meanwhile, $\beta = m\frac{2\pi}{L}$, and L is the length of the resonator. Thus,

$$m_i + m_s = 2m_p \tag{3.1}$$

Hence, *the momentum conservation agrees with mode number equidistant*. Thus, we choose the frequency domain to estimate the phase mismatch. Expand the frequency into Taylor series at ω_0 to the propagation constant β ,

$$\begin{aligned}
\omega_\mu &= \omega_0 + \frac{d\omega}{d\beta}(\beta_\mu - \beta_0) + \frac{1}{2} \frac{d^2\omega}{d\beta^2}(\beta_\mu - \beta_0)^2 + \dots \quad (3.2) \\
&= \omega_0 + \frac{d\omega}{d\beta} \frac{2\pi}{L} \mu + \frac{d^2\omega}{d\beta^2} \left(\frac{2\pi}{L} \mu \right)^2 + \dots \\
&= \omega_0 + D_1 \mu + D_2 \mu^2 + D_3 \mu^3 + \dots
\end{aligned}$$

where $D_1/2\pi = 1/v_g L$ is the *free spectrum range*, and

$$\text{as} = a$$